Human Tracheobronchial Basal Cells
Normal versus Remodeling/Repairing Phenotypes *In Vivo* and *In Vitro*

Moumita Ghosh[1]*, Shama Ahmad[1]*, Abhilasha Jian[1], Bilan Li[1], Russell W. Smith[1], Karen M. Helm[4], Max A. Seibold[1,2], Steven D. Groshong[3], Carl W. White[1‡], and Susan D. Reynolds[1‡]

[1]Department of Pediatrics, [2]Center for Genes, Environment, and Health, and [3]Department of Medicine, National Jewish Health, Denver, Colorado; and [4]University of Colorado Cancer Center, Anschutz Medical Campus, University of Colorado, Aurora, Colorado

Human tracheobronchial epithelial (TBE) basal cells (BCs) function as progenitors in normal tissue. However, mechanistic studies are typically performed *in vitro* and frequently use BCs recovered from patients who die of nonrespiratory disease. It is not known whether the cadaveric epithelium (*1*) is undergoing homeostatic remodeling and/or repair, or (*2*) yields BC clones that represent homeostatic processes identified in tissue. We sought to compare the phenotype of TBE-BCs with that of BCs cultured under optimal clone-forming conditions. TBE pathology was evaluated using quantitative histomorphometry. The cultured BC phenotype was determined by fluorescence-activated cell sorter analysis. Clone organization and cell phenotype were determined by immunostaining. The cadaveric TBE is 20% normal. In these regions, BCs are keratin (K)-5$^+$ and tetraspanin CD151$^+$, and demonstrate a low mitotic index. In contrast, 80% of the cadaveric TBE exhibits homeostatic remodeling/repair processes. In these regions, BCs are K5$^+$/K14$^+$, and a subset expresses tissue factor (TF). Passage 1 TBE cells are BCs that are K5$^+$/TF$^+$, and half coexpress CD151. Optimal clone formation conditions use an irradiated NIH3T3 fibroblast feeder layer (American Type Culture Collection, Frederick, MD) and serum-supplemented Epicult-B medium (Stemcell Technologies, La Jolla, CA). The TF$^+$/CD151$^-$ BC subpopulation is the most clonogenic BC subtype, and is enriched with K14$^+$ cells. TF$^+$/CD151$^-$ BCs generate clones containing BCs that are K5$^+$/Trp63$^+$, but K14$^-$/CD151$^-$. TF$^+$ cells are limited to the clone edge. In conclusion, clonogenic human TBE BCs (*1*) exhibit a molecular phenotype that is a composite of the normal and remodeling/reparative BC phenotypes observed in tissue, and (*2*) generate organoid clones that contain phenotypically distinct BC subpopulations.

CLINICAL RELEVANCE

Human basal cells (BCs) function as progenitors for tracheobronchial epithelial repair and regeneration. However, the mechanisms regulating BC function are typically evaluated *in vitro*. The impact of these mechanistic studies is limited by a lack of cross-referencing in tissue and cultured BC phenotype and function. We show that human tracheobronchial BC phenotypes are heterogeneous *in vivo*, and become more homogeneous *in vitro*. Highly clonogenic BCs generate organoid clones containing subregions that mimic the homeostatic remodeling/repair processes observed in the tracheobronchial epithelium.

Keywords: basal cell; remodeling; clonogenic frequency; phenotypic plasticity; stem cell

Basal cells (BCs) function as a progenitor for the human tracheobronchial epithelium (TBE) (1), and initiate *in vitro* cultures (2–4). BCs are identified on histological sections by staining for keratin (K). In mice, most steady-state tracheal BCs are K5$^+$/K15$^+$/K14$^-$, and only 20% of BCs are K5$^+$/K15$^+$/K14$^+$ (5). We showed that mouse BCs up-regulate K14 in response to naphthalene injury, and that nearly all BCs were K5$^+$/K15$^+$/K14$^+$ on Recovery Days 3–13 (5). These injury/repair studies suggested that the human BC phenotype may also vary as a function of tissue homeostasis or wounding. Our primary aim involved determining the K5/K14 profile of human TBE BCs.

Keratins are cytoplasmic proteins (6, 7). Consequently, viable respiratory BCs cannot be isolated on the basis of K expression. To overcome this issue, several groups identified cell-surface markers that can be used to separate BCs into subsets, using a fluorescence-activated cell sorter (FACS) (2, 3, 8–10). One of these markers, tissue factor (TF), is a component of the extrinsic coagulation cascade (11), and was originally developed for the isolation of nasal polyp BCs (12). We showed that all Passage 1 TBE BCs that were cultured in bronchial epithelial cell growth medium (BEGM) were TF$^+$, and that TF activity was necessary for BC survival *in vitro* (13). Other TBE BC markers include nerve growth factor receptor (2), podoplanin (14), CD49f (α6 integrin) (8), the tetraspanin CD151$^+$ (12), and Trp63 (p63) (15). Our secondary aim involved determining whether TF and CD151 were (*1*) expressed by TBE BCs, and (*2*) could be used to identify TBE BC subsets.

Our previous studies and those of others indicate that TBE repair in mice is mediated by BCs that proliferate and then differentiate to replace ciliated and secretory cell types (2, 5, 8, 14, 16–19). Human BC progenitor functions can also be evaluated *in vitro* (20). However, most analyses of human BCs have focused on the BC population as a whole, rather than on the

(*Received in original form January 30, 2013 and in final form July 2, 2013*)

* These authors contributed equally to this work.

‡ These authors contributed equally to this work.

This work was supported by National Institutes of Health grants RC1 HL099461 (S.D.R. and C.W.W.), RO1 HL075585 (S.D.R.), Supplement HL075585-S1 (S.D.R.), K18-HL107686 (M.G.), Young Clinical Scientist Award-Flight Attendants Medical Research Institute (M.G.), ES014448 (C.W.W.), and KL2RR025779 (S.A.). This research was also supported by the CounterACT Program, the Office of the Director at the National Institutes of Health, and National Institute of Environmental Health Sciences grant U54 ES015678 (C.W.W.). Foundation support was received from the Max and Yetta Karasik Family Foundation (C.W.W.). All FACS analyses were performed at the Flow Cytometry Shared Resource (University of Colorado Cancer Center), which is supported by National Institutes of Health award P30 CA 046934.

Author Contributions: M.G., S.A., A.J., K.M.H., C.W.W., and S.D.R. were responsible for the project's conception and design. M.G., S.A., A.J., B.L., R.W.S., K.M.H., M.A.S., S.D.G., C.W.W., and S.D.R. were responsible for the acquisition of data, or for the analysis and interpretation of data. M.G., S.A., K.M.H., M.A.S., S.D.G., C.W.W., and S.D.R. were responsible for drafting the article or revising it critically for important intellectual content. M.G., S.A., A.J., B.L., R.W.S., K.M.H., M.A.S., S.D.G., C.W.W., and S.D.R. were responsible for final approval of the version to be published.

Correspondence and requests for reprints should be addressed to Susan D. Reynolds, Ph.D., Department of Pediatrics, National Jewish Health, 1400 Jackson Street, K1007 Goodman Building, Denver, CO 80206. E-mail: reynoldss@njhealth.org

This article has an online supplement, which is accessible from this issue's table of contents at www.atsjournals.org

Am J Respir Cell Mol Biol Vol 49, Iss. 6, pp 1127–1134, Dec 2013

Originally Published in Press as DOI: 10.1165/rcmb.2013-0049OC on August 8, 2013
Internet address: www.atsjournals.org

identification/analysis of human BC subsets. Our third aim involved developing a culture method that allowed for the clonal analysis of human BCs, and determining whether the human BC population contains subsets with distinct clonogenic potential.

Mechanisms that regulate human BC proliferation and differentiation are frequently evaluated using cells that are recovered from subjects who die of nonrespiratory disease, and whose lungs are not used for transplantation (20). Kumar and colleagues demonstrated that the BC gene expression profile varies with culture condition (15). However, it remains unknown which, if any, of these culture conditions select for BCs that are phenotypically and/or functionally similar to BCs *in vivo*. Our final aim involved comparing the phenotypes of TBE BCs and organoids derived from highly colonogenic BCs.

MATERIALS AND METHODS

See the online supplement for more complete methods.

Human Tissues and Cells

Human tracheobronchial tissue was procured from the National Disease Research Interchange under protocols approved by the National Jewish Institutional Review Board. Subjects were 20- to 40-year-old accident victims who required minimal ventilator support, and who died of nonrespiratory disease. Respiratory parameters were defined as normal by the medical professional responsible for tissue procurement. TBE tissue from seven subjects was examined.

Human Tracheobronchial Cell Isolation and Culture

Cell were harvested and cultured in BEGM, as previously described (21, 22). For clonal studies, human tracheobronchial cells were cocultured on lethally irradiated (5,000 rad) NIH3T3 (American Type Culture Collection, Frederick, MD) feeder layers. Feeder cells were plated at 3×10^4 cells/cm^2. Cultures were maintained in BEGM, Gray's (generated in-house according to the formula in Ref. 23), or Epicult-B (24–26) media.

Immunofluorescence Experiments

Tissue sections were generated from formalin-fixed, paraffin-embedded tissue (27), and stained using previously described antibodies and methods (28). Other antibodies are listed in the online supplement. Epithelial pathology was quantified as previously indicated (5). Cytospin cell preparations were fixed and stained, and cell-type frequency was quantified as previously indicated (8).

Imaging

Nomarski images were acquired using an inverted Axiovert 40 CFL microscope and AxioVision software (Carl Zeiss, Inc., Thornwood, NY). For fluorescent imaging, tissue sections were imaged using a Zeiss AxioImager Z1 and Axiovision software (Carl Zeiss, Inc.). Cells and organoids were imaged using an AxioVert 200M microscope (Carl Zeiss, Inc.) equipped with a long working-distance ×10 objective and Slidebook software (Intelligent Imaging Innovations, Inc., Denver, CO).

FACS Analysis

One million Passage 1 tracheobronchial cells were incubated with αTF-FITC (American Diagnostica, Stamford, CT), αCD151-PE (BD Biosciences, San Diego, CA), αCD31-APC (eBioscience, San Diego, CA), αCD45-APC (eBioscience), and αCD90-APC (eBioscience) antibodies diluted in PBS containing 1% BSA (PBS/BSA) for 30 minutes at 4°C, and stained with 4′6-diamidino-2-phenylindole (DAPI). Nonimmune IgG1κ-APC and IgG1-FITC were used as isotype controls. Cell sorting was performed as previously indicated (8). Two different lasers were used to excite the FITC (488-nm) and phycoerythrin (568-nm) fluors (*see* Figure E3 in the online supplement). Sorted cells were reanalyzed for purity and viability.

Clone-Forming Cell Frequency Analysis

Clone-forming cell frequency (CFCF) was analyzed using the limiting dilution method (29). For the initial experiments, cells were delivered directly into the wells of 96-well plates, using twofold decrements from 500 cells/well to 1 cell/well. In subsequent experiments, sorted cells were directly deposited to the wells of 96-well plates, using a CyCLONE automated cloner (Cytomation, Fort Collins, CO). Twofold decrements from 128 cells/well to 1 cell/well were used. Each well was scored as positive or negative for colony formation. Linear regression analysis was used to determine the CFCF.

Statistical Analysis

Results are represented as means ± standard deviations. Differences were evaluated by the Student *t* test, using GraphPad Prism (Graphpad Software, La Jolla, CA).

RESULTS

The Cadaveric TBE Exhibits Homeostatic Remodeling and Repair

The presence or absence of apical cilia is often used to evaluate tissue pathology. Consequently, we immunostained TBE tissue for the ciliated cell marker acetylated tubulin (ACT). Similarly, BC frequency is used as an indicator of epithelial remodeling. We detected this cell type with the pan–BC marker K5. Four ACT/K5 staining patterns were detected in cadaveric TBE (Figure 1).

The "normal" pattern (Figure 1A) was defined by pseudostratification. In these regions, the luminal surface was defined by a continuous layer of ACT$^+$ cilia. K5$^+$ BCs were adjacent to the basement membrane, and their cell bodies defined a 2- to 3-cell-diameter subregion. The "hyperplastic" pattern (Figure 1B) was characterized by an increase in BC frequency (hyperplasia) and an interrupted row of apical cilia. The subregion defined by K5$^+$ BCs was expanded to 3–6 cell diameters, and some K5$^+$ cells were in contact with the airway lumen. The "disrupted" pattern (Figure 1C) was characterized by deficiencies in apical ACT$^+$ cilia and a patchy distribution of K5$^+$ BCs. Cells adjacent to the basement membrane were more densely packed than in normal regions, and some of these cells were K5$^-$. The "metaplastic" pattern (Figure 1D) was characterized by epithelial hyperplasia and a lack of apical cilia. Most epithelial cells were K5$^+$, and these cells exhibited a high nuclear to cytoplasmic ratio.

The frequency of each epithelial pattern was determined for each subject using stereological methods, and is presented as the volume frequency (Figure 1E). Epithelial pathology across subjects included normal (range, 0.00–32.95%; average, 17.4%), hyperplasic (range, 4.94–82.62%; average, 45.6%), disrupted (range, 0.00–50.92%; average, 20.6%), and metaplastic (range, 0–34.02%; average, 12.2%). The hyperplastic pattern was the most common, and was observed in all samples. The frequency of the hyperplastic pattern was increased relative to the normal ($P = 0.026$) and metaplastic ($P = 0.009$) patterns.

The mucous cell phenotype and metaplasia are also hallmarks of TBE remodeling. Because we showed that most normal airway secretory cells express the mucin Mucin 5B (MUC5B) (30), we evaluated the expression of this marker in the cadaveric TBE. Normal regions included MUC5B$^+$ cells whose cell bodies were contained within the epithelium, and a second subset that reached the luminal surface (Figure E1A). Hyperplastic and disrupted regions contained fewer MUC5B$^+$ cells than normal regions (Figures E1B and E1C). The majority of MUC5B$^+$ cells in these regions were luminal. Metaplastic regions contained very few MUC5B$^+$ cells (Figure 1D).

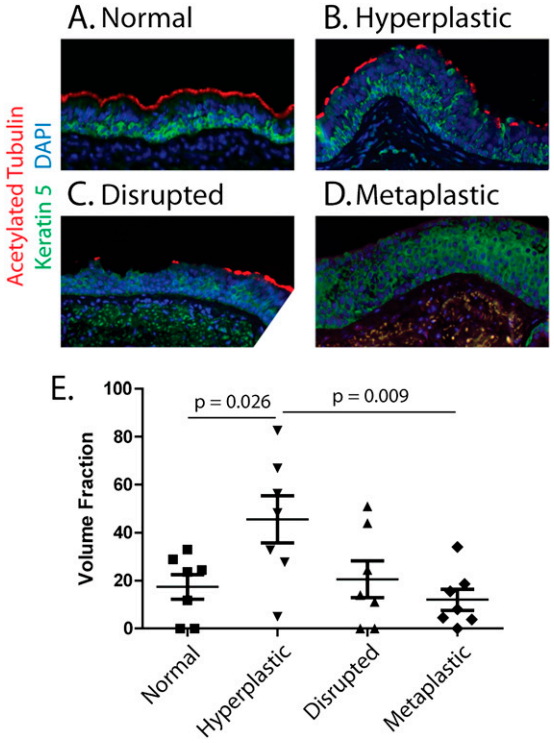

Figure 1. The cadaveric tracheobronchial epithelium undergoes remodeling and/or repair. (*A–D*) Tracheobronchial tissue from seven donors was stained for the ciliated cell marker acetylated tubulin (*red*) and the basal cell marker keratin (K)-5 (*green*). Nuclei were counterstained with 4′6-diamidino-2-phenylindole (DAPI) (*blue*). The epithelium was categorized into four morphological subtypes (*A*, normal; *B*, hyperplastic; *C*, disrupted; *D*, metaplastic). Representative images are shown at ×200 magnification. (*E*) The volume fraction of each epithelial subtype was determined using stereological methods. Data are presented as means ± SEMs ($n = 7$).

TBE Remodeling/Repair Correlates with Increased BC Proliferation

Our preliminary analysis indicated that very few MUC5B$^+$ cells coexpressed the proliferation marker Ki67 (MKI67 gene product that is detected by the Ki67 monoclonal antibody) (Figure E1). Consequently, we determined whether epithelial remodeling correlated with BC proliferation (Figure 2). Normal regions contained a rare population of K5$^+$/Ki67$^+$ cells that were located approximately one cell diameter apical to the basement membrane (Figure 2A). Hyperplasic regions contained an increased number of K5$^+$/Ki67$^+$ cells, relative to normal regions (Figure 2B). These mitotic BCs were located in a subregion that was approximately three cell diameters wide. Disrupted regions were characterized by the organization of K5$^+$/Ki67$^+$ cells into a distinct band that was 2–3 cell diameters wide (Figure 2C). BCs that were adjacent to the basement membrane and those that extended to the lumen were Ki67$^-$. Metaplastic regions contained K5$^+$/Ki67$^+$ cells that were distributed throughout the epithelium (Figure 2D). Importantly, K5$^+$/Ki67$^+$ cells included those adjacent to the basement membrane, as well as luminal cells.

K14 Is Up-Regulated in Areas of TBE Remodeling/Repair

To determine whether K14 expression varied as a function of TBE remodeling/repair, tissue sections were evaluated for the expression of K5 and K14. Normal regions contained rare K14$^+$ cells, and these cells expressed little or no K5 (Figure 3A). As previously

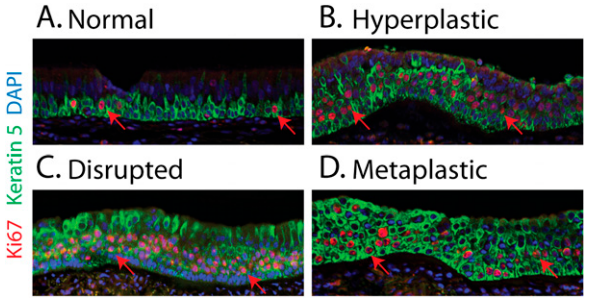

Figure 2. Epithelial remodeling/repair correlates with changes in basal cell proliferation. (*A–D*) Tracheobronchial tissue from seven donors was stained for the proliferation marker Ki67 (MKI67 gene product that is detected by the Ki67 monoclonal antibody) (*red*) and the basal cell marker K5 (*green*). Nuclei were counterstained with DAPI (*blue*). Representative images are shown at ×200 magnification. (*A*) Normal epithelial regions contained rare Ki67$^+$ cells (*arrows*). (*B–D*) Repair/remodeling regions contained increased numbers of Ki67$^+$ cells (*arrows*). The position of Ki67$^+$ cells differed from normal in hyperplastic regions (*B*) and disrupted (*C*) regions, and was random in metaplastic regions (*D*).

shown, hyperplasic regions contained rare K5$^+$ cells that extended to the luminal surface (Figures 1B and 2B). Most BCs in hyperplasic regions coexpressed K5 and K14 (Figure 3B). Disrupted regions contained frequent, luminal K5$^+$ cells (Figures 1C and 2C). As the frequency of luminal K5$^+$ cells increased (Figures 3B–3D), BCs that were adjacent to the basement membrane expressed more K14 than K5. Metaplastic regions contained BCs that coexpressed K5 and K14, as well as those that expressed only K5 (Figure 3D). The K5$^+$ cells were more luminal than the K5$^+$/K14$^+$ cells.

A Subset of TBE BCs Expresses TF

An immunofluorescence analysis demonstrated that TF was expressed predominantly in remodeling/reparative regions (Figure 4A) by K14$^+$ BCs that were adjacent to the basement membrane (Figures 4B and 4C), and by BCs that defined the normal (2–3 cell bodies) BC region (Figures 4A–4C and 4G). TF was not detected in BCs that were located in the more central or luminal

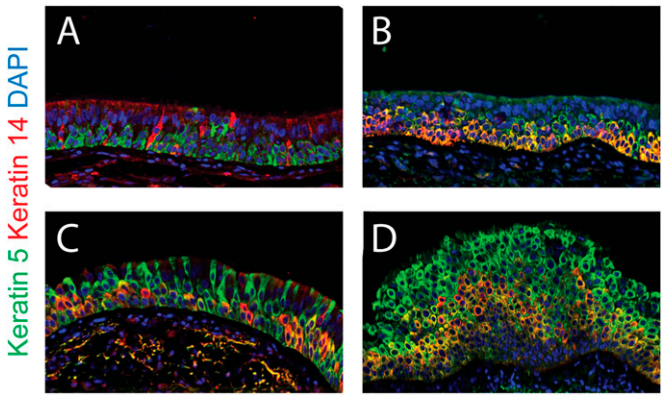

Figure 3. K14 is up-regulated in areas of epithelial remodeling and repair. (*A–D*) Tracheobronchial tissue from seven donors was stained for the basal cell markers K14 (*red*) and K5 (*green*). Nuclei were counterstained with DAPI (*blue*). Representative images are shown at ×200 magnification. (*A*) Normal epithelial regions contained rare K14$^+$ cells. (*B–D*) Remodeling/reparative regions contained increased numbers of K14$^+$ cells that were enriched within epithelial subregions adjacent to the basement membrane. *B*, hyperplastic; *C*, disrupted; *D*, metaplastic.

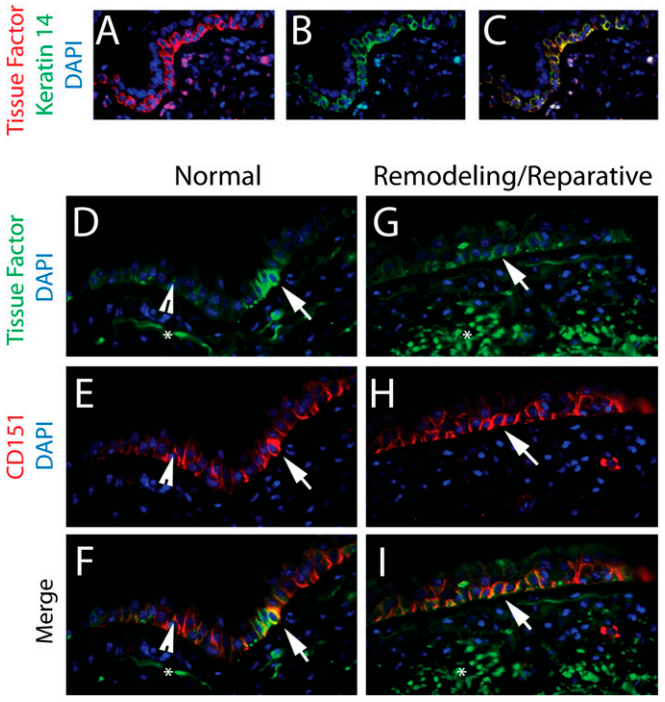

Figure 4. Differential expression of tissue factor (TF) and tetraspanin CD151. (*A–C*) Tracheobronchial tissue from seven donors was stained for TF (*red*) and the basal cell marker K14 (*green*). Nuclei were counterstained with DAPI (*blue*). Split color images (*A* and *B*) and a merged image (*C*) are depicted. Representative images are shown at ×200 magnification. (*D–I*) Tracheobronchial tissue from seven donors was stained for TF (*green*) and CD151 (*red*). Nuclei were counterstained with DAPI (*blue*). (*D*, *E*, *G*, and *H*) Split color images. (*F* and *I*) Merged images. Representative images for normal regions (*D–F*) and reparative/remodeling regions (*G–I*) are shown at ×200 magnification. *Arrowheads*, $TF^-/CD151^+$ cells. *Arrows*, $TF^+/CD151^+$ cells.

subregions of hyperplasic, disrupted, or metaplastic regions (not shown). Some normal regions contained small clusters of TF^+ BCs that were adjacent to the basement membrane (Figure 4D).

A Subset of TBE BCs Expresses Tetraspanin (CD151)

An immunofluorescence analysis showed that CD151 was expressed by BCs in normal regions (Figure 4E), including the TF^+ subset. CD151 was enriched on the lateral and apical surfaces of BC bodies that were adjacent to the basement membrane. CD151 was not detected on more luminal BC bodies. In remodeling/reparative regions, CD151 was limited to BC bodies that were adjacent to the basement membrane (Figure 4H). Most of these cells coexpressed TF (Figure 4I).

Irradiated Fibroblast Feeders and Serum Promote BC Clone Formation *In Vitro*

Variations in BC phenotypes *in vivo* and the potential for distinct progenitor activities among BC subsets indicated that TBE BC function should be evaluated by clonal analysis. In preparation for these experiments, we cultured TBE BCs under standard conditions (collagen IV–coated tissue culture plastic and serum-free BEGM medium), and evaluated TBE BC viability as a function of seeding density. A significant trend toward decreased viability was noted at low cell density (Figure 5A).

To improve cell viability in low cell density cultures, we compared the ability of various culture media and conditions to

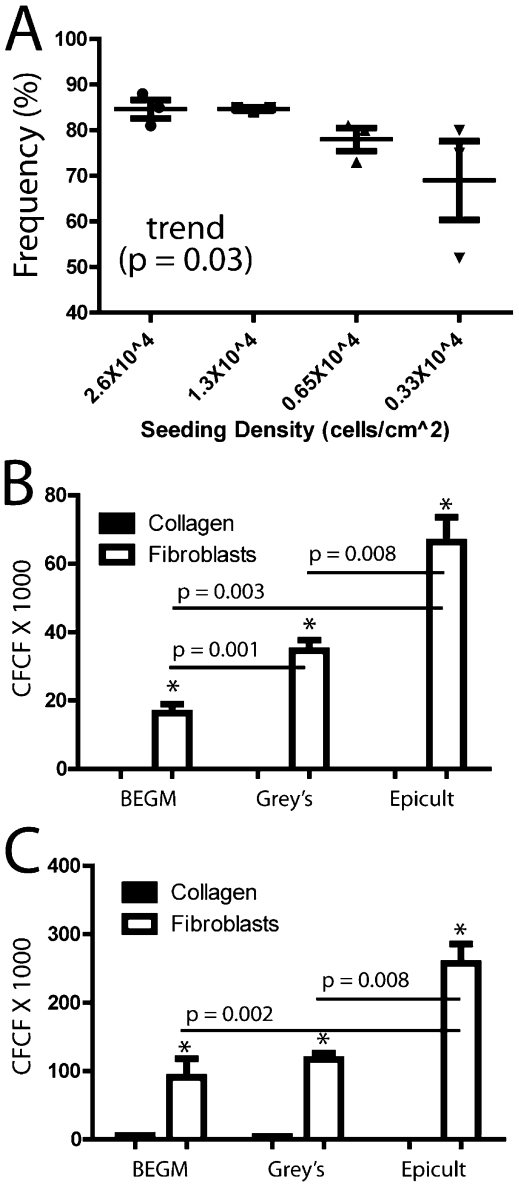

Figure 5. Irradiated fibroblast feeders and serum promote basal cell (BC) clone formation. (*A*) Passage 1 tracheobronchial BCs were seeded at various densities in serum-free bronchial epithelial cell growth medium (BEGM) medium. Cell viability was analyzed on culture Day 5 by DAPI exclusion and fluorescence-activated cell sorter analysis. Data are presented as means ± SEMs ($n = 3$). (*B* and *C*) Multiwell plates (96-wells) were coated with collagen IV or seeded with an irradiated NIH3T3 fibroblast feeder layer (American Type Culture Collection, Frederick, MD). Passage 1 tracheobronchial BCs were seeded at various cell inputs (500 to 1 cell/well, six wells/dilution) and cultured in (*B*) serum-free BEGM, Gray's medium, or Epicult-B medium (Stemcell Technologies, La Jolla, CA), or (*C*) media supplemented with 5% FBS. The clone-forming cell frequency (CFCF) was determined on Day 7. Data are presented as means ± SEMs ($n = 3$). *$P < 0.05$ relative to collagen.

support TBE BC clone formation. Initial experiments compared CFCF in Passage 1 TBE BCs that were cultured in serum-free BEGM, Gray's, or Epicult-B media. Collagen-coated plastic or an irradiated NIH3T3 fibroblast feeder layer was used. This experiment demonstrated that an irradiated NIH3T3 fibroblast feeder layer increased CFCF in all media, and that maximal CFCF was achieved in Epicult-B medium (Figure 5B). The CFCF was further increased when fibroblast feeder layers were

used in conjunction with FBS-containing BEGM, Gray's, and Epicult-B media (Figure 5C). The TBE BC CFCF was greatest when cells were cultured on irradiated NIH3T3 fibroblasts in FBS-containing Epicult-B medium.

All Passage 1 TBE BCs Express α6 Integrin (CD49f)

To determine the phenotype of TBE BCs that are used to model human lung disease, we cultured Passage 1 tracheobronchial cells to 80% confluence, using the BEGM method. Cells were recovered by trypsinization and stained for hematopoietic (CD45), endothelial (CD31), and mesenchymal (CD90) markers. Viable epithelial cells were defined by side scatter and forward scatter (FSC) (Figures 6A and E2A), FSC height and FSC width (Figures 6B and E2B), the exclusion of the DNA dye DAPI, and negativity for CD45, CD31, and CD90 (Figures 6C and E2C). This experiment demonstrated that 95% ± 5% ($n = 6$ donors) of viable, Passage 1 tracheobronchial cells were epithelial cells.

Because we previously reported that the CD49f expression level could be used to define subsets of mouse BCs (8), we evaluated the expression of this marker in TBE BCs (Figures E2D and E2E). This experiment demonstrated that all TBE BCs expressed CD49f, and that the CD49f expression level does not vary among TBE BCs. Thus, variations in CD49f expression level could not be used to define subsets of Passage 1 TBE BCs.

Aldehyde Dehydrogenase Activity Does Not Distinguish Clonogenic TBE BCs

Aldehyde dehydrogenase (ALDH) activity has been used to identify lung cancer stem cells (31), as well as mouse (8, 32) and human (32) respiratory BC subsets. ALDH activity is evaluated using the fluorescent ALDH substrate Aldefluor (Stem Cell Technologies, Vancouver, BC, Canada) and FACS analysis. TBE BCs were identified as already indicated (Figure E2), and cells with low and high ALDH activity were identified by comparisons of Aldefluor intensity in the absence or presence of the inhibitor diethylaminobenzaldehyde (Figures E2F and E2G). $ALDH^{high}$ cells comprised 3.25% of all TBE BCs (Figure E2G).

To determine whether $ALDH^{low}$ and $ALDH^{high}$ cells exhibited distinct clonogenic potential, we isolated these cell populations using a conservative gating strategy (Figure E2G), and determined their CFCF using the limiting dilution method (29). The CFCF for $ALDH^{low}$ cells was 7.89 ± 2.83, and the CFCF for $ALDH^{high}$ cells was 9.58 ± 1.75. These values were not significantly different.

TF and CD151 Define Subsets of TBE BCs *In Vitro*

We next evaluated the expression of TF and CD151 in Passage 1 TBE cells from three donors. An analysis of TF demonstrated that 99% ± 2% of Passage 1 TBE cells were TF^+ (Figures 6D–6G and E3). The TF^+ population was sorted, deposited onto glass slides, and stained for K5 and K14. Quantification demonstrated that all TF^+ cells were $K5^+$ BCs (Figure 6G). Interestingly, half of the $TF^+/K5^+$ BCs coexpressed K14 (Figure 6G). TF^+ cells did not express ciliated or mucous cell differentiation markers (13). FACS analysis showed that only approximately 25% of TF^+ cells coexpressed CD151 (Figures 6D–6F and 6H). Thus, Passage 1 TBE BCs contained two subsets that were defined by their expression of K14 and/or CD151.

Clonogenic TBE BCs Are Enriched in the $TF^+/CD151^-$ Subpopulation

We next determined whether the $TF^+/CD151^+$ and $TF^+/CD151^-$ BC subsets contained different frequencies of clonogenic cells. Passage 1 cells from three donors were sorted into the wells of 96-well plates containing irradiated NIH3T3 fibroblast feeder layers, and cultured in Epicult-B medium supplemented with

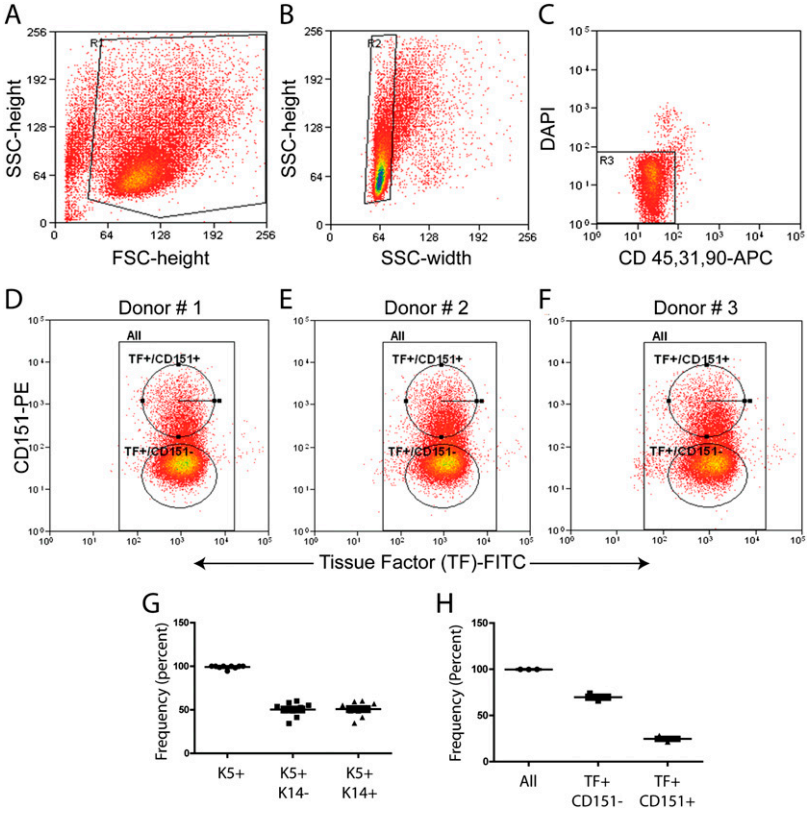

Figure 6. Separation of Passage 1 tracheobronchial basal cells into subsets. (*A–D*) Fluorescence-activated cell sorter separation of Passage 1 tracheobronchial cells. (*A*) Cells were identified by side scatter (SSC) and forward scatter (FSC), as indicated by the *black outline*. (*B*) Single cells were identified by SCC height and width, as indicated by the *black outline*. (*C*) Viable cells ($DAPI^-$) and nonhematopoietic (CD45), nonendothelial (CD31), and nonfibroblast (CD90) cells were identified as indicated by the *black outline*. APC, allophycocyanin. (*D–F*) Epithelial cells were separated into two subsets, according to the expression of tetraspanin CD151 and TF. *Black outlines* indicate epithelial cells (All), $TF^+/CD151^+$ populations, and $TF^+/CD151^-$ populations. (*G*) Cells from each subpopulation were sorted, deposited phycoerythrin on glass slides, and stained for the basal cell markers K5 and K14. The frequency of cells expressing one or both keratins was determined by counting three fields from each of three donors. Data are presented as means ± SEMs ($n = 9$). (*H*) The frequencies of epithelial, TF^+CD151^-, and $TF^+/CD151^+$ cells were determined. Data are presented as means ± SEMs ($n = 3$).

5% FBS. The CFCF for unfractionated BCs and $TF^+/CD151^+$ cells was similar (Figure 7A). The selection of $TF^+/CD151^-$ cells resulted in a 2.5-fold enrichment of clonogenic cells, and the CFCF was significantly increased relative to unfractionated BCs and the $TF^+/CD151^+$ ($P < 0.001$) populations.

Dual immunofluorescence analysis of cytospin preparations confirmed that all Passage 1 TBE BCs expressed K5 (13) (not shown). Staining for K14 demonstrated that approximately 40% of unfractionated cells or TF^+CD151^+ cells coexpressed K14 (Figure 7B). In contrast, the selection of $TF^+/CD151^-$ cells resulted in a 1.5-fold enrichment of $K14^+$ cells (Figure 7B; $P < 0.001$). Linear regression analysis of CFCF versus $K14^+$ cell frequency indicated a significant relationship ($R^2 = 0.096$) between these parameters (Figure 7C).

Clone Morphology and Cellular Composition

The structural characteristics of clones generated by $TF^+/CD151^-$ cells were evaluated by Nomarski microscopy (Figures 7D–7F). Most clones were round. Some clones contained a region of high cell density at their perimeter and a central region composed of flattened cells (Figure 7F). All clone cells were $K5^+$ (Figure 7G), and most clone cells were $Trp63^+$ (Figure 7H). Surprisingly, K14 was not detected (Figures 7I and E4B, positive control).

The $K5^+/K14^-$ phenotype suggested that the clone-forming cells had reverted to the "normal phenotype" detected *in vivo*. To evaluate this finding further, clones were stained for TF and CD151. Wide-field microscopy suggested that TF^+ cells were localized to the perimeter of the clone (Figure 7J). This finding was confirmed using Z-stacks and deconvolution software (Figure 7K). In contrast to the normal phenotype, all clone cells were $CD151^-$ (Figures 7L and E4A, positive control). Thus, $TF1^+/CD151^-$ cells generated organoid clones in which perimeter cells were $TF^+/CD151^-$, and central cells were $TF^-/CD151^-$.

DISCUSSION

TBE Remodeling/Repair and TBE BC Phenotype

We show that cadaveric tracheobronchial tissue, which is commonly used as a source of human BCs, is lined by an epithelium containing normal regions and regions undergoing homeostatic remodeling/repair. Surprisingly, the majority of the epithelium is involved in remodeling and/or repairing. This pathology was unexpected, because the subjects' respiratory parameters were defined as "normal" by a medical professional. These results suggest that standard clinical parameters are insensitive indicators of TBE remodeling/repair.

The remodeling/repair pathology provided an opportunity to correlate BC phenotype with pathological status. Normal TBE BCs are $K5^+/K14^-$ and $CD151^+/TF^-$, and present a low mitotic index. These BCs likely perform homeostatic functions, which

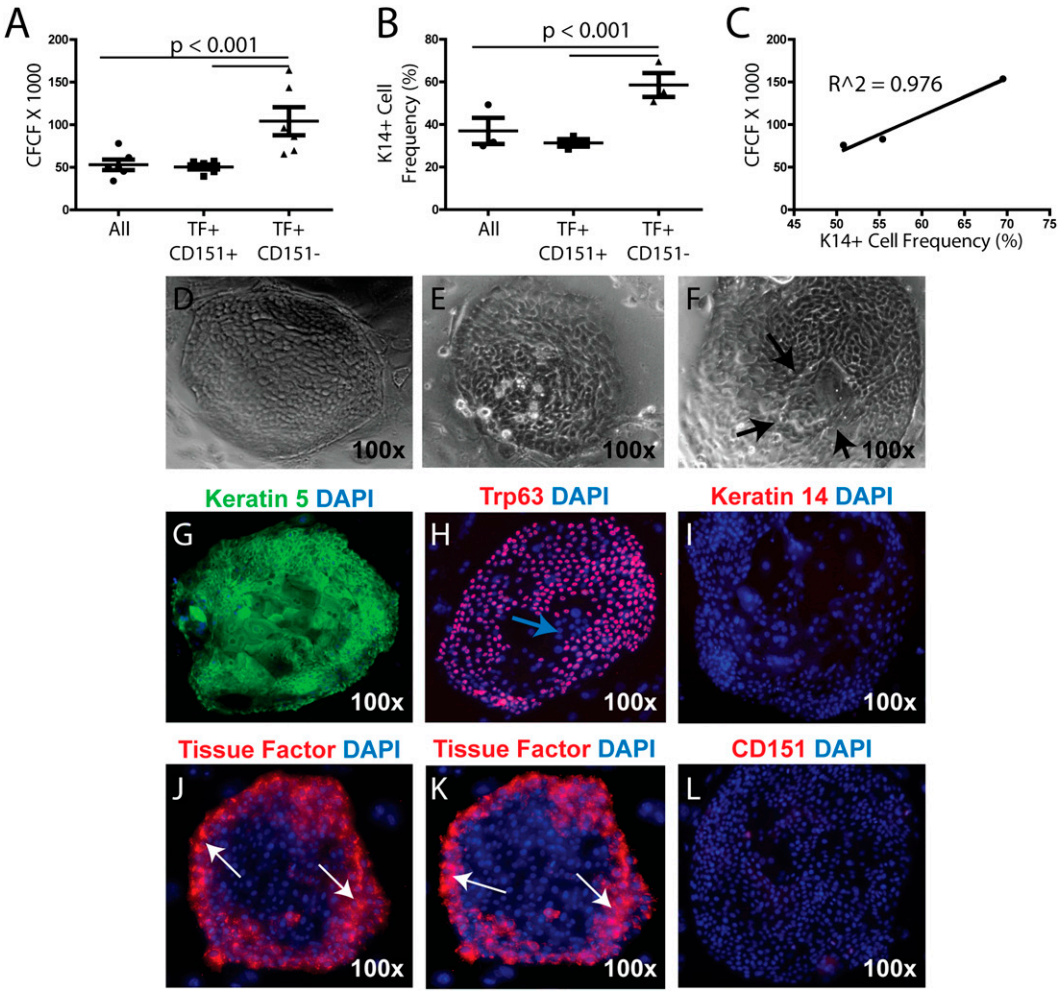

Figure 7. $TF^+/CD151^-$ cells comprise the most clonogenic basal cell subtype *in vitro*, and generate organoid clones. (*A–C*) Passage 1 tracheobronchial basal cells separated into epithelial (All), $TF^+/CD151^+$, or $TF^+/CD151^-$ subpopulations. (*A*) Multiwell plates (96-wells) were seeded with an irradiated NIH3T3 fibroblast feeder layer. Cells from each subpopulation were seeded at various cell inputs (128 to 1 cell/well, six wells/dilution), and cultured in Epicult-B medium supplemented with 5% FBS. Clone forming cell frequency (CFCF) was determined on Day 7. Data are presented as means ± SEMs ($n = 3$ donors, two determinations/donor). (*B*) Cells from each subpopulation were deposited onto glass slides, and stained for K14. The frequency of $K14^+$ cells was determined by counting three fields/population/donor. Data are presented as means ± SEMs ($n = 3$). (*C*) The relationship between the CFCF and $K14^+$ cell frequency was determined by linear regression analysis ($R^2 = 0.976$). (*D–F*) Nomarski images of $TF^+/CD151^-$ cell–derived clones. (*F*) *Arrows* indicate the low cell density observed in some clones. Representative images of three clone types are presented. (*G–L*) Fluorescent imaging of representative clones stained for DAPI (*blue*) and (*G*) K5 (*green*), (*H*) Trp63 (*red*), (*I*) K14 (*red*), (*J* and *K*) TF (*red*), or (*L*) CD151. Positive controls for K14 and CD151 are described in Figure E2. (*J*) Merged Z-stack. (*K*) Deconvoluted Z-stack image. *Blue arrow* in *H* indicate $Trp63^-$ cells. *White arrows* in *J* and *K* indicate tissue factor–positive cells.

may include epithelial attachment, metabolism, and immunomodulation (33).

BCs in remodeling/reparative regions coexpress K5 and K14. Consistent with our analysis of mouse tracheal BCs (5), the expression of K14 by human BCs correlates with increased BC proliferation. BCs in these regions can be further categorized on the basis of TF expression. BCs that make extensive contact with the basement membrane are $K5^+/K14^-/CD151^+/TF1^+$, and exhibit a low mitotic index. BCs with less basement membrane contact tend to be $K5^+/K14^+/CD151^-/TF^-$, and to exhibit an increased mitotic index. These data support our previous conclusion that TF expression was associated with human BC survival and the establishment of a proliferative BC pool *in vitro* (13). However, these data also suggest that TF expression decreases as TBE BCs enter the cell cycle *in vivo*.

Clonogenic BC Subtype

We tested a series of previously reported cell surface markers for their ability to define clonogenic subsets of TBE BCs. We showed that (*1*) TF and CD151 can be used to define subsets of TBE BCs that are cultured according to the BEGM method, and (*2*) $TF^+/CD151^-$ cells comprise the most clonogenic BC subset. In agreement with the tissue analysis, $K14^+$ cells are enriched in the clonogenic population. However, TF expression distinguishes the clonogenic cells detected *in vitro* from mitotic cells in tissue.

We found that CD49f was uniformly expressed by TBE BCs. Thus, in contrast with mouse BCs (8), this marker could not be used to define subsets of human TBE BCs. We also reported that ALDH activity levels distinguished mouse BC subsets (8), and others used this marker to define subsets of human TBE cells (32). We detected ALDH activity in TBE BCs. However, when we used the inhibitor diethylaminobenzaldehyde to select $ALDH^{high}$ and $ALDH^{low}$ subsets, we were unable to detect a difference in clone formation. The discrepancy between the present analysis and the previous report may be attributable to differences in cell preparation methods (differential cell recovery versus total TBE cell recovery) and/or cell cultures (freshly isolated cells versus Passage 1 cells). Based on our mouse studies, we suggest that ALDH activity must be used in conjunction with other markers to define subsets of BCs.

Optimal Culture Conditions

We show that cell viability is decreased at low cell density in BEGM cultures. Thus, TF up-regulation may reflect a stress response to culture conditions. TF is a component of the extrinsic coagulation cascade, and BCs express some, but not all, clotting cascade components (13). Thus, serum-free culture conditions may be deficient in critical cascade components needed to fully activate the extrinsic coagulation cascade and cell survival. This notion is supported by the finding that culture in FBS-containing BEGM improves clonogenic cell frequency. Further, the coagulation cascade is regulated by endothelial and mesenchymal tissue *in vivo* (11). The finding that culturing on an irradiated fibroblast feeder layer improves clone formation in BEGM suggests that the full utilization of the extrinsic coagulation cascade by BCs is facilitated by interactions with non-epithelial cells such as fibroblasts.

We showed that TBE BC clone formation is optimal for cells that are cultured on irradiated NIH3T3 feeder layers in Epicult-B medium supplemented with 5% FBS. The Epicult-B method is superior to cultures with feeders in BEGM/FBS, and moderately superior to cultures with feeders in Gray's medium/FBS. The Epicult-B medium was originally formulated for the growth of mammary progenitor cells in monoculture, and was not previously tested for epithelial–fibroblast cocultures. Additional studies are needed to determine whether the growth advantage detected in Epicult-B was dattributable to effects on the BC progenitors, the fibroblast feeders, and/or interactions between the two cell types.

$TF^+/CD151^-$ Clones Mimic the Homeostatic Remodeling/Repair Observed in Tissue

$TF^+/CD151^-$ cells that were cultured using the Epicult-B method generated clones that were composed of $K5^+/Trp63^+$ BCs. Interestingly, the clone perimeter was composed of TF^+ cells that were adjacent to the fibroblast layer. This location may mimic the normal position of TF^+ cells adjacent to the basement membrane in tissue, and indicate that fibroblast–BC interactions induce this phenotype.

We also show that all clone cells were $K14^-/CD151^-$. Thus, highly clonogenic $TF^+/CD151^-$ cells down-regulated K14 when cultured, but they did not express a completely "normal" phenotype. Previous studies correlated CD151 expression with early-stage differentiation *ex vivo* and *in vitro* (3). We confirmed this finding (data not shown). Thus, we suspect that the Epicult-B method suppresses early differentiation, and we suggest that this method will be valuable for analyses of clonogenic BC progenitors.

Author disclosures are available with the text of this article at www.atsjournals.org.

Achnowledgments: The authors thank Robert J. Mason, M.D., for defining normal respiratory parameters and the selection of TBE tissue for use in these experiments. The contents are the authors' sole responsibility and do not necessarily represent the official views of the National Institutes of Health.

References

1. Engelhardt JF, Schlossberg H, Yankaskas JR, Dudus L. Progenitor cells of the adult human airway involved in submucosal gland development. *Development* 1995;121:2031–2046.
2. Rock JR, Onaitis MW, Rawlins EL, Lu Y, Clark CP, Xue Y, Randell SH, Hogan BL. Basal cells as stem cells of the mouse trachea and human airway epithelium. *Proc Natl Acad Sci USA* 2009;106:12771–12775.
3. Hajj R, Baranek T, Le Naour R, Lesimple P, Puchelle E, Coraux C. Basal cells of the human adult airway surface epithelium retain transit-amplifying cell properties. *Stem Cells* 2007;25:139–148.
4. Dvorak A, Tilley AE, Shaykhiev R, Wang R, Crystal RG. Do airway epithelium air–liquid cultures represent the *in vivo* airway epithelium transcriptome? *Am J Respir Cell Mol Biol* 2011;44:465–473.
5. Cole BB, Smith RW, Jenkins KM, Graham BB, Reynolds PR, Reynolds SD. Tracheal basal cells: a facultative progenitor cell pool. *Am J Pathol* 2010;177:362–376.
6. Hutton E, Paladini RD, Yu QC, Yen M, Coulombe PA, Fuchs E. Functional differences between keratins of stratified and simple epithelia. *J Cell Biol* 1998;143:487–499.
7. Omary MB, Ku NO. Cell biology: skin care by keratins. *Nature* 2006;441: 296–297.
8. Ghosh M, Helm KM, Smith RW, Giordanengo MS, Li B, Shen H, Reynolds SD. A single cell functions as a tissue-specific stem cell and the *in vitro* niche-forming cell. *Am J Respir Cell Mol Biol* 2011;45: 459–469.
9. Hegab AE, Ha VL, Gilbert JL, Zhang KX, Malkoski SP, Chon AT, Darmawan DO, Bisht B, Ooi AT, Pellegrini M, *et al.* A novel stem/progenitor cell population from murine tracheal submucosal gland ducts with multipotent regenerative potential. *Stem Cells* 2011;29: 1283–1293.
10. Avril-Delplanque A, Casal I, Castillon N, Hinnrasky J, Puchelle E, Péault B. Aquaporin-3 expression in human fetal airway epithelial progenitor cells. *Stem Cells* 2005;23:992–1001.
11. Rao LV, Mackman N. Factor VIIa and tissue factor: from cell biology to animal models. *Thromb Res* 2010;125:S1–S3.
12. Dupuit F, Gaillard D, Hinnrasky J, Mongodin E, de Bentzmann S, Copreni E, Puchelle E. Differentiated and functional human airway

epithelium regeneration in tracheal xenografts. *Am J Physiol Lung Cell Mol Physiol* 2000;278:L165–L176.
13. Ahmad S, Ahmad A, Rancourt RC, Neeves KB, Loader JE, Hendry-Hofer T, Di Paola J, Reynolds SD, White CW. Tissue factor signals airway epithelial basal cell survival via coagulation and par1/2. *Am J Respir Cell Mol Biol* 2013;48:94–104.
14. Rock JR, Gao X, Xue Y, Randell SH, Kong YY, Hogan BL. Notch-dependent differentiation of adult airway basal stem cells. *Cell Stem Cell* 2011;8:639–648.
15. Kumar PA, Hu Y, Yamamoto Y, Hoe NB, Wei TS, Mu D, Sun Y, Joo LS, Dagher R, Zielonka EM, *et al*. Distal airway stem cells yield alveoli *in vitro* and during lung regeneration following H1N1 influenza infection. *Cell* 2011;147:525–538.
16. Brechbuhl HM, Ghosh M, Smith MK, Smith RW, Li B, Hicks DA, Cole BB, Reynolds PR, Reynolds SD. β-catenin dosage is a critical determinant of tracheal basal cell fate determination. *Am J Pathol* 2011;179:367–379.
17. Ghosh M, Brechbuhl HM, Smith RW, Li B, Hicks DA, Titchner T, Runkle CM, Reynolds SD. Context-dependent differentiation of multipotential keratin 14–expressing tracheal basal cells. *Am J Respir Cell Mol Biol* 2011;45:403–410.
18. Hong KU, Reynolds SD, Watkins S, Fuchs E, Stripp BR. Basal cells are a multipotent progenitor capable of renewing the bronchial epithelium. *Am J Pathol* 2004;164:577–588.
19. Hong KU, Reynolds SD, Watkins S, Fuchs E, Stripp BR. *In vivo* differentiation potential of tracheal basal cells: evidence for multipotent and unipotent subpopulations. *Am J Physiol Lung Cell Mol Physiol* 2004;286:L643–L649.
20. Bernacki SH, Nelson AL, Abdullah L, Sheehan JK, Harris A, Davis CW, Randell SH. Mucin gene expression during differentiation of human airway epithelia *in vitro*: MUC4 and MUC5B are strongly induced. *Am J Respir Cell Mol Biol* 1999;20:595–604.
21. Ahmad S, Ahmad A, Dremina ES, Sharov VS, Guo X, Jones TN, Loader JE, Tatreau JR, Perraud AL, Schöneich C, *et al*. BCL-2 suppresses sarcoplasmic/endoplasmic reticulum Ca^{2+}-ATPase expression in cystic fibrosis airways: role in oxidant-mediated cell death. *Am J Respir Crit Care Med* 2009;179:816–826.
22. Fulcher ML, Gabriel S, Burns KA, Yankaskas JR, Randell SH. Well-differentiated human airway epithelial cell cultures. *Methods Mol Med* 2005;107:183–206.
23. Widdicombe JH, Sachs LA, Morrow JL, Finkbeiner WE. Expansion of cultures of human tracheal epithelium with maintenance of differentiated structure and function. *Biotechniques* 2005;39:249–255.
24. Eirew P, Stingl J, Raouf A, Turashvili G, Aparicio S, Emerman JT, Eaves CJ. A method for quantifying normal human mammary epithelial stem cells with *in vivo* regenerative ability. *Nat Med* 2008;14:1384–1389.
25. Lindvall C, Evans NC, Zylstra CR, Li Y, Alexander CM, Williams BO. The Wnt signaling receptor Lrp5 is required for mammary ductal stem cell activity and Wnt1-induced tumorigenesis. *J Biol Chem* 2006;281:35081–35087.
26. Stingl J, Eaves CJ, Zandieh I, Emerman JT. Characterization of bipotent mammary epithelial progenitor cells in normal adult human breast tissue. *Breast Cancer Res Treat* 2001;67:93–109.
27. Smith RW, Hicks DA, Reynolds SD. Roles for β-catenin and doxycycline in the regulation of respiratory epithelial cell frequency and function. *Am J Respir Cell Mol Biol* 2012;46:115–124.
28. Cole BB, Smith RW, Jenkins KM, Graham BB, Reynolds PR, Reynolds SD. Tracheal basal cells: a facultative progenitor cell pool. *Am J Pathol* 2010;177:362–376.
29. Taswell C. Limiting dilution assays for the determination of immunocompetent cell frequencies: I. Data analysis. *J Immunol* 1981;126:1614–1619.
30. Seibold MA, Smith RW, Urbanek C, Groshong SD, Cosgrove GP, Brown KK, Schwarz MI, Schwartz DA, Reynolds SD. The idiopathic pulmonary fibrosis honeycomb cyst contains a mucocilary pseudostratified epithelium. *PLoS ONE* 2013;8:e58658.
31. Moreb JS. Aldehyde dehydrogenase as a marker for stem cells. *Curr Stem Cell Res Ther* 2008;3:237–246.
32. Hegab AE, Ha VL, Darmawan DO, Gilbert JL, Ooi AT, Attiga YS, Bisht B, Nickerson DW, Gomperts BN. Isolation and *in vitro* characterization of basal and submucosal gland duct stem/progenitor cells from human proximal airways. *Stem Cells Transl Med* 2012;1:719–724.
33. Evans MJ, Van Winkle LS, Fanucchi MV, Plopper CG. Cellular and molecular characteristics of basal cells in airway epithelium. *Exp Lung Res* 2001;27:401–415.